Published in final edited form as:

Nat Chem Biol. 2017 March ; 13(3): 325–332. doi:10.1038/nchembio.2283.

Enzyme-Catalyzed Cationic Epoxide Rearrangements in Quinolone Alkaloid Biosynthesis

Yi Zou[†], **Marc Garcia-Borràs**[‡], **Mancheng C. Tang**[†], **Yuichiro Hirayama**[#], **Dehai H. Li**[&], **Li Li**[†], **Kenji Watanabe**[#], **K. N. Houk**[*,‡], and **Yi Tang**[*,†,‡]

[†]Department of Chemical and Biomolecular Engineering, University of California, Los Angeles, CA90095, United States

[‡] Department of Chemistry and Biochemistry, University of California, Los Angeles, CA90095, United States

[&] Key Laboratory of Marine Drugs, Chinese Ministry of Education, School of Medicine and Pharmacy, Ocean University of China, Qingdao, 266003, P. R. China

[#] Department of Pharmaceutical Sciences, University of Shizuoka, Shizuoka 422-8526, Japan

Abstract

Epoxides are highly useful synthons and biosynthons in the construction of complex natural products during total synthesis and biosynthesis, respectively. Among enzyme-catalyzed epoxide transformations, a notably missing reaction, compared to the synthetic toolbox, is cationic rearrangement that takes place under strong acids. This is a challenging transformation for enzyme catalysis, as stabilization of the carbocation intermediate upon epoxide cleavage is required. Here, we discovered two Brønsted acid enzymes that can catalyze two unprecedented epoxide transformations in biology. PenF from the penigequinolone pathway catalyzes a cationic epoxide rearrangement under physiological conditions to generate a quaternary carbon center, while AsqO from the aspoquinolone pathway catalyzes a 3-*exo*-tet cyclization to forge a cyclopropane-tetrahydrofuran ring system. The discovery of these new epoxide-modifying enzymes further highlights the versatility of epoxides in complexity generation during natural product biosynthesis.

[*]Corresponding author: yitang@ucla.edu, houk@chem.ucla.edu.

AUTHOR CONTRIBUTIONS

Y.Z., M.G.-B., K.N.H. and Y.T. developed the hypothesis and designed the study. Y.Z. performed all *in vivo* and *in vitro* experiments as well as compound isolation and characterization. M.C.T., D.H.L. Y.H. and L.L. performed compound characterization. M.G.-B. and K.N.H. performed the computational experiments. All authors analyzed and discussed the results. Y.Z., M.G.-B., K.W., K.N.H., and Y.T. prepared the manuscript.

COMPETING FINANCIAL INTERESTS

The authors declare no competing financial interests.

ADDITIONAL INFORMATION

Supplementary information is available in the online version of the paper. Correspondence and requests for materials should be addressed to Y.T. or K. N. H.

INTRODUCTION

Epoxides are versatile building blocks for synthesis of complex organic molecules.[1, 2] Due to considerable ring strain of the three-membered cyclic ether and the polarized oxygen-carbon bonds, epoxides can be subjected to ring opening in regioselective and stereoselective fashions using a large variety of synthetic catalysts.[3-11] In natural product biosynthetic pathways, epoxides are strategically introduced by Nature to serve as an electrophilic functional group.[2, 12, 13] During polyether biosynthesis, tandem opening of epoxides under general acid/general base catalysis can lead to formation of fused or bridged five- and six-membered cyclic ethers (Fig. 1a).[14, 15] An epoxide is also regioselectively positioned to initiate the cascade of ring closing steps during terpene cyclization. Presentation of an active site Brønsted acid to the epoxide by terpene cyclases (TCs) leads to concerted epoxide cleavage and C-C bond formation, as exemplified in the biosynthesis of lanosterol from 2,3-oxidosqualene,[16] indole diterpenes[17, 18] and meroterpenoids[19] (Fig. 1a). Enzymes that can modify epoxides have been developed into industrial biocatalysts, including the use of epoxide hydrolases (EHs) and haloacid dehalogenases (HADs) in the optical resolution of pharmaceutical building blocks.[20, 21] The recent engineering of squalene-hopene cyclase (SHC) as a protonase towards the chiral synthesis of cyclohexanols further highlights the interests towards finding new enzymatic tools that can be used in the transformation of epoxide synthons.[22]

Notwithstanding the impressive regio- and stereoselective control of EHs and TCs, the range of enzymatic epoxide transformations is severely limited compared to established synthetic methodologies. Notably, the widely used acid-catalyzed cationic rearrangement of epoxides in the presence of strong Lewis and Brønsted acids, such as the Meinwald, semi-pinacol, and Jung rearrangements has no known counterpart in biology.[23-26] These rearrangement reactions can generate richly functionalized 1, 2-difunctional ring-opened products and quaternary carbons, and have been prominently featured in keys steps of total syntheses.[27] The use of strong acids is required for the S_N1-like ring opening of the epoxide and formation of the carbocation, which under anhydrous conditions can lead to migration of substituents to form aldehydes and ketones (Fig. 1b). In contrast, under biological conditions, formation of a cationic intermediate is more challenging; instead a concerted protonation/addition mechanism in TCs is invariably observed. Therefore, in order for an enzyme active site to catalyze a cationic epoxide rearrangement reaction, three requirements must be satisfied: 1) the presence of a Brønsted acid that is sufficiently acidic to protonate the epoxide; 2) a discrete C-O cleavage step without anchimeric assistance from proximal nucleophiles such as olefins and hydroxyl groups; and 3) sufficient stabilization of the resulting carbocation without quenching by water or enzyme side chains to enable the rearrangement reaction to occur.

Our efforts to discover new enzymatic epoxide transformations are guided by natural products that have unusual oxygen-containing heterocycles not present in most epoxide-derived compounds such as polyethers. The quinolone alkaloid family of fungal natural products contains several members that have such structural features, including the diastereomeric pairs of penigequinolone A (**1a**) and B (**1b**) from *Penicillium sp.* and aspoquinolone A (**2a**) and B (**2b**) from *Aspergillus nidulans* (Fig. 1c).[28-31] The two pairs of

compounds contain the identical quinolone core but differ in the cyclization of the oxidized ten-carbon prenyl side chain. The vinylic tetrahydropyran (THP) of **1** contains a quaternary carbon, while the same linear fragment in **2** has been cyclized into an unusual vinylic cyclopropane-tetrahydrofuran (THF) 3,5-ring system.[32] Both **1** and **2** have been proposed to derive from the epoxide **5**,[33] however the responsible enzymes have not been discovered. Here we show that in each pathway, an enzyme with conserved domain similarity to CrtC (carotenoid 1,2 hydratase) is responsible for a biologically unprecedented epoxide rearrangement. We demonstrate that the enzymes PenF and AsqO can catalyze a cationic epoxide rearrangement and a 3-*exo*-tet cyclization to yield penigequinolone A/B (**1**) and aspoquinolone A/B (**2**), respectively. Our findings not only expand the enzymatic repertoire for epoxide modification, but further underscore the importance of epoxides as versatile biosynthons in natural product biosynthesis.

RESULTS

Functional parallel between the *pen* and *asq* pathways

The *pen* pathway in *Penicillium thymicola* involves a key intermediate **4**, which contains a ten-carbon, hydroxylated prenyl chain (Fig. 1c).[31] Analysis of the *pen* and *asq* biosynthetic pathways showed that nearly all genes in the two pathways leading to **4** are conserved (Supplementary Results, Supplementary Table 1),[31,34] suggesting the two pathways share the same transformations and intermediates. Comparison of the remaining enzymes in the two pathways revealed three pairs of homologous enzymes as shown in Fig. 1c. These include a membrane-bound flavin-dependent monooxygenase (FMO) (PenE and AsqG, Supplementary Fig. 1), an epoxide hydrolase (EH) like enzyme (PenJ and AsqB), and an enzyme with conserved domain homology to carotenoid or kievitone hydratase (CrtC superfamily protein) (PenF and AsqC). We had shown that in the *pen* pathway, the FMO PenE catalyzes the epoxidation of **4** to yield **5**, which can spontaneously undergo 5-*exo*-tet cyclization to yield the THF **6**.[31] This transformation is accelerated in the presence of the EH PenJ.[31] To compare the functions of the FMO and EH enzymes in the two pathways, we performed a biotransformation assay by feeding **4** into yeast cultures expressing different combination of *pen* and *asq* FMO and/or EH. In all cases, the complete conversion of **4** to THF **6** was demonstrated (Supplementary Fig. 2). These results confirmed that the FMO and EH pair in the two pathways are functionally equivalent to afford **6,** which has been proposed to undergo rearrangement to afford **1**.[33] Also in these mixand-match experiments, formation of the 6-*endo*-tet product **7** from **5** was not observed as previously proposed for the *asq* pathway (Fig. 1c).[33]

PenF catalyzes the Meinwald rearrangement

PenF (362 aa) and AsqC (347 aa) share low sequence homology to CrtC but contain a conserved domain motif (Supplementary Fig. 3). The CrtC family of enzymes catalyze the addition of water to a carbon-carbon double bonds, including the best characterized carotenoid 1,2-hydratase CrtC of which the family is named after.[35] The CrtC from *Rubrivivax gelatinosus* was characterized to have an active site aspartic acid that is proposed to protonate the terminal double bond of lycopene,[35] in the same mechanism as that of squalene-hopene cyclase.[36] Beyond lycopene hydration, it is unknown what additional

catalytic functions are accessible from members of the CrtC family. Sequence alignment showed the conserved acidic amino acid residue (Glu in PenF and Asp in AsqC, Supplementary Fig. 3) is present in both enzymes. In the absence of additional enzyme candidates, we initially propose the homologous pair of PenF and AsqC in the two pathways may catalyze the conversion of **6** to **1** and **2**, respectively. Indeed, the Δ*penF* mutant of *P. thymicola* was abolished in production of **1**, and accumulated only **6** (Supplementary Fig. 4).

To biochemically test the functions of PenF or AsqC, we performed both yeast-based biotransformation and *in vitro* reaction using purified FLAG-tagged enzymes (Supplementary Fig. 5). AsqC was cloned from cDNA obtained from overexpression of the gene in *A. nidulans* A4 since the *asq* cluster is silent in the original host (Supplementary Fig. 6). However, when PenF or AsqC was added to **6**, no consumption of **6** was observed using either enzyme (Supplementary Fig. 7). To examine if **6** is an on-pathway intermediate of **1**, we supplied either **3** (Fig. 1c), which is an upstream on-pathway intermediate, or **6** to an early-stage blocked mutant (*ΔpenN*, NRPS) of *P. thymicola*. Whereas **3** readily restored the biosynthesis of **1**, feeding of **6** did not lead to any detectable formation of **1** (Supplementary Fig. 8). Hence these results refute the previous hypothesis that **6** is the penultimate precursor of **1** (Fig. 1c), but rather indicate **6** is an off-pathway product. Our experimental observations that **6** can be readily formed from **5**, and has a dedicated EH in both *pen* and *asq* pathways, are consistent with the isolation of **6** as a cometabolite from all producing strains of **1** and **2**.[29, 30]

We then reconsidered alternative reactions that can lead to formation of **1**. The presence of the quaternary carbon 8 (C8) in **1** suggests that a rearrangement of the carbon connectivities is required if starting from **5** (Fig. 1c). This corresponds to the Meinwald or Jung rearrangement that takes place during cationic epoxide rearrangement (Fig. 1b). We hypothesized that PenF, with its active site Glu serving as the Brønsted acid, may catalyze such a reaction. To test this hypothesis, we added 20 μM PenF to the *in vitro* reaction mixture containing 0.4 mM **4** and microsomal PenE (from 20 mg/ml total protein concentration) in the presence of FAD and NADPH. The reaction mixture was extracted, analyzed by LC-MS to show that most of **4** was converted to a new product **8** (*m/z* 482 [M-H]$^-$), with <1% of products converted to the S_N2 product **6** (Fig. 2, ii). Excluding PenF led to near complete conversion to **6** as expected (Fig. 2, i). By comparing to an authentic standard, **8** was verified to be the hemiacetal yaequinolone D which contains the quaternary C8 (Fig. 2, ii and vi). To complete the biosynthetic pathway of **1**, we cloned and expressed a SDR-like reductase PenD encoded in the *pen* cluster (Supplementary Fig. 5). Addition of PenD and NADPH to **8** led to the complete conversion to **1** (Fig. 2, iii), thereby confirming **8** is indeed an on-pathway intermediate. No reaction is observed in the absence of NADPH. PenD therefore catalyzes both the dehydration of **8** and the reduction of the resulting oxonium to yield **1** (Fig. 3). To demonstrate the conversion from **4** to **1**, co-incubation of **4** with PenE, PenF and PenD in the presence of FAD and NADPH led to formation of **1** (Fig. 2, iv and vii).

Our results demonstrate PenF indeed catalyzes the cationic rearrangement of epoxide **5** into **8**. The proposed mechanism for this transformation is shown in Fig. 3. The conserved Glu

residue in PenF is proposed to serve as a Brønsted acid and presents the acidic proton to the epoxide hydrogen. This leads to cleavage of the C-O bond to yield a tertiary carbocation. This cationic species then undergoes the 2,3-carbon migration to form the new C6-C8 bond and the protonated aldehyde, which can be attacked by the C3-OH to yield hemiacetal **8**. Whereas Lewis acids such as $BF_3{\cdot}Et_2O$ are used to promote synthetic Meinwald and Jung reactions, PenF does not require any divalent cations as cofactors. Assay in the presence of 10 mM EDTA did not lead to reduction of enzyme activity (Supplementary Fig. 9a). The essential role of the Glu residue towards PenF function was verified through site-directed mutagenesis to Ala, which nearly completely abolished the formation of intermediate **8** (Supplementary Fig. 9a).

Remarkably in the presence of PenF, formation of THF **6** is essentially completely suppressed. The formation of **6** from **5** via S_N2 attack of the anchimeric hydroxyl group is in agreement with Baldwin's rules and is highly favorable under general acid/general base conditions. We performed Density functional theory (DFT) calculations to explore the different epoxide transformations using the epoxide-allylic alcohol fragment of **5** as a model substrate (Supplementary Fig. 10). As expected under general acid/general base catalysis, the 5-*exo*-tet reaction is favored over 6-*endo*-tet with $\Delta\Delta G^{\ddagger}$ = 2.1 kcal/mol (Fig. 4). Under general acid catalysis, the 6-*endo*-tet transition state Gibbs energy is lower than those of 5-*exo*-tet and C8-O cleavage by 1.1 kcal/mol and 3.7 kcal/mol, respectively (Fig. 4). However, in the presence of PenF, no trace of either 5-*exo*-tet product **6** or 6-*endo*-tet product **7** can be detected (Fig. 2, ii). Thus, PenF is able to suppress 5-*exo*-tet and 6-*endo*-tet cyclization reactions allowing only the formation of the carbocation as a result of the C8-O bond cleavage. PenF can control that reactivity by binding the substrate in a conformation to prevent the anchimeric assistance of the C3 hydroxyl group or by suppressing the general acid/general base catalysis. From the carbocation, DFT calculations confirmed that the subsequent carbon bond migration is energetically easy with a barrier of $\Delta G^{\ddagger}$ = 5.6 kcal/mol. The resulting aldehyde is 7 kcal/mol more stable (Supplementary Fig. 11). In addition, the cyclization of the aldehyde to form the 6-membered ring intermediate is also an exergonic process ($\Delta G = -8$ kcal/mol), indicating that these reaction steps are also highly thermodynamically favorable to generate the cyclic precursor **8** of **1**.

AsqC is a dehydratase

Having completed the biosynthetic pathway of **1**, we next investigated if the unusual 3,5-ring system in **2** can be formed from **5** in the presence of the PenF homolog AsqC. Recombinant AsqC was added to the *in vitro* assay including **4** and yeast microsomes containing AsqG. Whereas AsqG alone led to the formation of **6**, addition of AsqC resulted in the complete conversion of **4** into two new compounds **9** (*m/z* 448 $[M\text{-}H]^-$) and **10** (*m/z* 464 $[M\text{-}H]^-$) (Fig. 5a, i and ii), both with a red-shifted λ_{max} from 323 nm to 340 nm. To obtain sufficient amounts of **9** and **10** for structural characterization, we constructed a *P. thymicola* Δ*penF::*P*gpdA-asqC* mutant in which *penF* was deleted and replaced with an *asqC* overexpression cassette (Supplementary Fig. 6). Consistent with the *in vitro* assay, the strain produced both **9** and **10** (Supplementary Fig. 12). Isolation of **9** and **10** following large scale fermentation enabled complete characterization of the compound to be the C3

dehydrated derivatives of **4** and **5**, respectively (Supplementary Note 1). In contrast to **5**, **10** is highly stable and no spontaneous rearrangement of any kind can be observed in buffer.

The formation of **9** and **10** suggests that the AsqC catalyzes the C3-dehydration reaction, which represents to the reverse of the hydration reaction catalyzed by CrtC. To investigate the relative timing of AsqG-catalyzed epoxidation and AsqC-catalyzed dehydration reactions, we directly added **4** to AsqC which led to the rapid and complete conversion to **9** (Fig. 5a, iii). In the absence of AsqC, we could detect slow and spontaneous dehydration of **4** to two products (Fig. 5a, iv), one of which corresponded to **9** while the other was likely the *exo* methylene product. In the presence of AsqC, only **9** is observed indicating regioselective dehydration under enzymatic conditions. Addition of microsomal AsqG to **9** did not lead to formation of the epoxide **10** (Fig. 5a, v), suggesting AsqG can only use **4** as substrate while AsqC has more substrate promiscuity in recognizing both **4** and **5**. Establishing the substrate specificity of AsqG also indicates that **10** is an on-pathway intermediate, while **9** is a shunt metabolite. Notably, although AsqC is shown to catalyze a different reaction using **5** compared to PenF, both enzymes are able to completely suppress the formation of **6**, further highlighting the role of the enzyme active site in redirecting the reaction pathway of the epoxide substrate.

Further evidence of PenF-catalyzed epoxide rearrangement

With the stable dienyl epoxide **10** in hand, we tested the substrate tolerance of PenF towards the dehydrated side chain. A direct assay with an epoxide substrate can further validate the proposed cationic rearrangement activity of PenF. We expected PenF to catalyze the C-O bond cleavage of **10** to yield a tertiary carbocation, which can result in 2,3-carbon bond migration to yield the quaternary aldehyde product **11** (Fig. 3). Gratifyingly, direct incubation of **10** with PenF in Tris buffer (pH 7.4) led to the formation of a new product with *m/z* 464 $[M\text{-}H]^-$ expected for **11** (Fig. 5b, i and ii). Considering the aldehyde can be readily reduced under *in vivo* fermentation conditions, we opted to scale up the *in vitro* reaction using purified PenF. Purification of the new product followed by NMR analysis confirmed the structure to be **11** (Supplementary Note 1). To compare the function of PenF to the synthetic Meinwald reaction, we performed a direct reaction of **10** in the presence of the Lewis acid $BF_3{\cdot}Et_2O$. Interestingly, complete conversion of **10** to two products was observed (Supplementary Fig. 13a), including the aldehyde **11** (70%) and a new product **12** (30%). DFT computations using a dienyl truncated carbocation revealed that the hydrogen atom shift from C7 to C8 to give a ketone derivative has a $\Delta G^{\ddagger}$ = 3.2 kcal/mol, very low and only 2 kcal/mol higher than the Meinwald rearrangement barrier (Supplementary Fig. 13b). NMR characterization of **12** (Supplementary Note 1) showed the product to be indeed the ketone that derives from an H-shift of a carbocation. Therefore, formation of **11** by PenF unequivocally confirms PenF can catalyze the Meinwald-like reaction previously only accessible through strong Lewis or Brønsted acids (when triflic acid was used, **10** rapidly degraded). The exclusive selectivity towards 2,3-migration to form **11** over **12** also shows that PenF is involved in dictating the outcome of the cationic rearrangement.

AsqO catalyzes 3-*exo*-tet cyclization of 10 to form 2

Elucidation of AspC as a dehydratase that affords **10** moves the biosynthetic pathway one step closer to the product **2**. We hypothesize that the cyclopropyl ring in **2** may be formed from a 3-*exo*-tet cyclization of **10** to yield a cationic intermediate (Fig. 3). The cyclopropylcarbinyl cation is then quenched by the tertiary C8 hydroxyl group, a reaction that can be accelerated with the *gem*-dimethyl group at C8 to furnish the THF ring and complete the biosynthesis of **2**.[37] A few synthetic examples of using 3-*exo*-tet cyclization to forge the 3,5-ring system in natural products have been reported.[38-40] In the synthesis of mycorrhizin A, strong Lewis acids such as $BF_3{\cdot}Et_2O$ or Brønsted acids such as triflic acid were used to generate a tertiary carbocation, which is the site of attack by the double bond.[38] C-O cleavage is unlikely to be involved in transforming **10** to **2** as formation of a secondary carbocation is required. Instead, we propose a concerted attack of the anchimeric C3-C4 double bond on C7 under Brønsted acid catalysis to forge the new C4-C7 bond. Therefore, the involvement of an additional enzyme with similar active site configuration to PenF would be required.

To identify the *asq* enzyme that may catalyze this unusual epoxide rearrangement, we carefully reanalyzed the *asq* gene cluster deposited in NCBI for any misannotated open reading frames. The *asqI* gene was initially annotated to encode a hemocyanin homolog fusion to a C-terminal protein with an unusually large intron at the fusion junction (Supplementary Fig. 14). Reannotation together with analysis of cDNA sequence from overexpressed *asqI* revealed the C-terminal fusion is in fact encoded on a separate open reading frame (Supplementary Figs. 5 and 14). Interestingly, the reannotated gene *asqO* encodes a CrtC homolog that is weakly homologous to PenF (identity/similarity: 39%/45%), but contains the conserved Asp residue found the CrtC family (Supplementary Fig. 3). This raises an interesting possibility that this additional CrtC-like enzyme can catalyze the 3-*exo*-tet reaction. Soluble AsqO (365 aa) was expressed and purified from yeast as a FLAG-tagged enzyme (Supplementary Fig. 5). When 20 μM AsqO was added to **10** in Tris buffer, partial conversion to the diastereomeric mixture of **2** can be confirmed using an authentic standard of **2** isolated from the producing strain of *A. nidulans* HKI0410 (Fig. 5b, iii and v). The ratio of the two forms of **2** (~4:1) from the in vitro reaction is similar to the ratio of **2a** and **2b** isolated from the producing organism as an inseparable mixture. To probe the catalytic mechanism of AsqO, we mutated the conserved Asp at the active site which led to complete loss of activity (Supplementary Fig. 9b). This is consistent with our proposal that a catalytic Brønsted acid in AsqO is required to initiate the cyclization reaction. Interestingly, whereas PenF could not catalyze the transformation of **10** to **2** under the same condition (Fig. 5b, ii), addition of AsqO and AsqG to **4** led to ~20% conversion of **4** to **8**, with the remaining forming **6** (Fig. 5b, iv).

DISCUSSION

In this work, we elucidated the complete biosynthetic pathways of penigequinolone **1** and aspoquinolone **2**, and uncovered the functions of three enzymes belonging to the CrtC superfamily. We showed that PenF can catalyze the cationic rearrangement of epoxides into the corresponding aldehydes. AsqO catalyzes an enzymatic 3-*exo*-tet cyclization to yield the

cyclopropyl-THF ring system in **2**, using the substrate **10** derived from the dehydration of **5** catalyzed by AsqC. Although all three enzyme-catalyzed reactions are not previously associated with the CrtC family, which performs hydration of double bonds, the proposed reaction mechanisms of PenF and AsqO are consistent with the use of a Brønsted acid in the active site as in CrtC. The discovery of PenF and AsqO greatly expands the scope of epoxide transformations accessible through enzyme catalysis. In particular, PenF is the first biochemically characterized enzyme that catalyzes a cationic epoxide rearrangement, which has been suggested to take place in several biosynthetic pathways.[41-44] The new chemistry of PenF enables enzymatic forging of quaternary carbon centers starting with epoxide substrates, which is a notable application of the synthetic reaction. [3, 10, 11, 23, 25, 26, 27]

We propose a carboxylic acid from the side chain of a conserved active site residue, Glu and Asp in PenF and AsqO, respectively, serves as the Brønsted acid. The use of the strongly acidic proton has been noted in other enzymes, most notably in squalene-hopene cyclase (HSC), oxidosqualene cyclase (OSC) and CrtC.[35, 36, 45] In HSC and CrtC, the challenging protonation of the substrate double bond is performed via the *anti*-oriented Asp acidic proton through a specialized amino acid network that includes a protonated histidine side chain that polarizes the Asp acid carbonyl, and a hydrogen-bonded water molecule that bridges the carboxylated oxygen and a tyrosine side chain.[16, 35, 45] In OSC, the more readily protonated epoxide receives a less acidic *syn* proton from Asp that is hydrogen-bonded to two Cys residues.[16, 36] Surprisingly, although PenF and AsqO do not show homology to either HSC or OSC, the active site region displays high sequence homology to CrtC (Supplementary Fig. 3), thereby suggesting the use of a more acidic environment by these two enzymes to initiate the rearrangement of epoxide substrates.

Despite the common use of a strong active site Brønsted acid, PenF and AsqO catalyze completely different, yet seemingly competing reactions starting with **10**. AsqO is mechanistically similar to OSC and engineered HSC[22] for concerted epoxide opening (C7-O cleavage) and C4-C7 bond formation. However, PenF appears to be truly unique in its function to 1) suppress such concerted epoxide opening; 2) promote C8-O bond cleavage that forms a carbocation intermediate; and 3) direct the regioselective 2,3-migration in Meinwald rearrangement. DFT calculations on a model dienyl epoxide indicate that the two reactions have comparable energy barriers, with the concerted C7-O cleavage and C4-C7 bond formation disfavored by 1 kcal/mol with a model general acid catalysis (Fig. 4). Therefore, the active sites of PenF and AsqO must bind and interact with **10** in drastically different ways. Intriguingly, the active site residues of PenF are different compared to all other CrtC homologs (Supplementary Fig. 3). PenF has an active site Glu instead of the conserved Asp residue in all other CrtC homologs. Glu has one additional methylene unit, and may position the acidic side chain and the substrate epoxide in a slightly different conformation. This may lead to cation-**π** interactions with the multitude of tryptophan residues in PenF. Furthermore, the conserved Tyr that forms hydrogen bond network in the active sites of SHC and CrtC is substituted with a histidine (His) in PenF. While histidine may remain part of the H-bond network in PenF, depending on its protonation state and positioning relative to the catalytic Glu and epoxide, it may serve to promote the protonation of the epoxide during the C8-O cleavage and stabilization of the carbocation intermediate

formed (Supplementary Fig. 3). Indeed, mutation of Glu to Asp in PenF greatly decreased the activity of PenF towards dienyl epoxide **10** and resulted in only trace amounts of aldehyde **11** detected, while mutation of His to Ala completely abolished the activity of PenF (Supplementary Fig. 9a). Hence a subtle alteration (one methylene less) in positioning of the Brønsted acid can have a profound impact on the product outcome. The exact roles of the catalytic residues will be identified with ongoing X-ray crystallographic studies.

Using DFT calculations, we also examined an alternative pathway to form aspoquinolone **2** from dienyl epoxide **10** (Supplementary Fig. 15). In the first step, concerted protonation, hydrogen shift from C6 to C7 and double bond migration forms the C3 tertiary carbocation. A required *trans* to *cis* isomerization of the C4-C6 double bond can then lead to quenching of the cation by the C8 hydroxyl group to yield an oxepane intermediate. Further hydrogen shift and cyclopropane formation can yield **2**. However, high reaction barriers make this pathway inaccessible under normal conditions, making 3-*exo*-tet the only viable mechanism for the formation of **2**. The elucidated enzymatic synthesis of **2** also warrants reexamination of the stereochemistry of the pair of diastereomeric products. Both **2a** and **2b** were initially isolated as inseparable mixtures, and mixed stereochemistries were assigned at C4 and C7. While it is expected that *syn* relative stereochemistry is present at these two carbons, we suggest that the mixed stereochemistry is in fact at C3 (Fig. 3). This is because we expect the epoxidation step by AsqG to be stereospecific (either *S* or *R*, in squalene 2,3-oxidase it is *S*)[46], while the spontaneous quenching of the cation to **2** (calculated $\Delta G = -10.1$ kcal/mol, Supplementary Fig. 16) to be nonstereoselective. Unfortunately, due to the activity of AsqO being suboptimal compared to that of PenF, re-isolation and NMR characterization of **2** was not possible in this study.

Our discovery expands the role of epoxide as a biosynthon in generation of structural complexity in natural products. Since double bonds are frequently oxidized into epoxides in biosynthesis, we expect that additional CrtC homologs that catalyze carbon rearrangements can be discovered. Indeed, using PenF and AsqO as leads, we identified >40 candidate genes that show 35% to 70% similarity to PenF and AsqO from sequenced fungal genomes (Supplementary Fig. 17a). Interestingly, a majority of these homologs are distributed among plant pathogens, such as *Fusarium* sp., *Colletotrichum* sp., *Trichoderma* sp., *Valsa* sp. and *Cochliobolus* sp. as well as animal pathogens such as *Metarhizium* sp. and *Pseudogymnoascus* sp. Moreover, many homologs are clustered with natural product biosynthetic gene clusters, such as the one containing PKS20 in the highly pathogenic *Cochliobolus heterostrophus* C5 (Supplementary Fig. 17b).[47] In addition, a FMO or P450 enzyme is found in most of these identified gene clusters, perhaps serving as the two or one-electron enzyme manifold for epoxidation, respectively. None of the identified pathways has an associated product, further justifying the potential of using homologs of PenF and AsqO to mine pathways that may produce compounds of new structures.

In conclusion, by targeting the biosynthesis of two quinolone alkaloids from fungi, we discovered two enzymes that can catalyze two unprecedented epoxide transformations in biology. The reactions described here, such as the Meinwald rearrangement, have significant utility in organic synthesis. With the discovery of new enzymes that can specifically perform

such reactions, we have set the stage to engineer the substrate specificities towards applications in chiral synthesis and biocatalysis.

ONLINE METHODS

Fungal strains and culture condition

P. thymicola IBT 5891 was obtained from the IBT culture collection (Kgs. Lyngby, Denmark). *A. nidulans* FGSC A4 and *A. nidulans* FGSC A1145 was obtained from Fungal Genetics Stock Center (http://www.fgsc.net/). *P. thymicola* was maintained on PDA (potato dextrose agar, BD) 5 days for sporulation or liquid PDB medium (PDA medium without agar) and SDA (Sabouraud Agar, BD) for gene over-expression, genomic DNA and RNA extraction. *A. nidulans* was maintained on CD agar for sporulation, or liquid CD-ST medium for gene over-expression, genomic DNA and RNA extraction (http://www.fgsc.net/). *P. thymicola* were maintained on SDA at 24°C, 7 days for the production of penigequinolone A/B.

General DNA manipulation techniques

E. coli TOP10 and *E. coli* XL-1 were used for cloning, following standard recombinant DNA techniques. DNA restriction enzymes were used as recommended by the manufacturer (New England Biolabs, NEB). PCR was performed using Q5® High-Fidelity DNA Polymerase (NEB). PCR products were confirmed by DNA sequencing. *E. coli* BL21(DE3) (Novagen) was used as the *E. coli* host for protein expression. *Saccharomyces cerevisiae* strain BJ5464-NpgA (MATα ura3-52 his3-Δ200 leu2-Δ1 trp1 pep4::HIS3 prb1 Δ1.6R can1 GAL) was used as the yeast host for protein expression.

Gene Knock-out and over-expression in *P. thymicola* and *A. nidulans*

The gene *penF* was deleted in *P. thymicola* based on previous hygromycin split-marker apporach,[31] and the polyethylene glycol-mediated protoplast transformation of *P. thymicola* and *A. nidulans* was performed. Genes *asqC*, *asqG* and *asqO* according to the new annotations were amplified from the gDNA of *A. nidulans* FGSC A4, cloned into different over-expression plasmids and introduced into *P. thymicola* mutants or *A. nidulans* FGSC A1145 (Supplementary Fig. 6). The genotypes of all mutants were verified by PCR. The plasmids and primers used are listed in Supplementary Tables 2 and 3. Polyethylene glycol-mediated protoplast transformation of i) *P. thymicola* was performed to introduce *penF* knock-out cassette or *asqG* and *asqC* over-expression cassette, or ii) *A. nidulans* FGSC A1145 was performed to introduce *asqO* over-expression cassette. Briefly, *P. thymicola* or *A. nidulans* FGSC A1145 germinated cells were collected, washed twice with osmotic medium (1.2 M $MgCl_2$, 10 mM sodium phosphate, pH 5.8) and resuspended in enzyme cocktail solution (3 mg/mL Lysing Enzymes, 3 mg/mL Yatalase in osmotic medium) at 28°C for 8 hours. After wash twice with STC buffer, protoplasts were gently mixed with DNA and incubated for 1 hour on ice. 500 °L of PEG 4000 solution (60% PEG 4000, 50 mM $CaC1_2$, 50 mM Tris-HCI, pH 7.5) was added for 100 μL protoplast mixture, incubated at room temperature for 20 min and plated on regeneration selection medium i) PSA, PDA agar supplemented with 1.2 M sorbitol, 100 μg/mL hygromycin B for *penF* knock-out and 100 μg/mL zeocin for *asqC* and *asqG* over-expression; ii) CDS, CD agar supplemented with 1.2

M sorbitol, 0.5 μg/mL pyridoxine HCl, 10 mM uridine and 5 mM uracil for *asqO* over-expression. After incubation at room temperature for about 4 days, the *P. thymicola* transformants were transferred into fresh 2 mL PDB medium at 24°C, 200 rpm, 2 days, the *A. nidulans* A1145 transfromatants were transferred into fresh 2 mL liquid CD medium (supplemented with 0.5 μg/mL pyridoxine HCl, 10 mM uridine and 5 mM uracil) at 37°C, 200 rpm, 2 days. Mycelia were collected, lyophilized and grounded to disrupt cells. Cell lysate was solubilized in LETS buffer (10 mM Tris-HCl, pH 8.0, 20 mM EDTA, 0.5% SDS, 0.1 M LiCl) and extracted twice with phenol/chloroform. Genomic DNA was precipitated with ethanol, and resuspended in H_2O. The genotypes of *penF* mutant, *asqG*, *asqC* and *asqO* over-expression mutant were verified by PCR.

Chemical analysis and compound isolation

For small-scale analysis, the *P. thymicola* wild-type and correct transformants were grown on PDA or SDA agar for 7 days at 24°C. 1 cm × 1 cm agar was extracted with 2 ml acetone, and then evaporated to dryness. The dried extracts were dissolved in 300 μl methanol for LC-MS analysis. All LC-MS analyses were performed on a Shimadzu 2020 EVLC-MS (Kinetex™ 1.7 μm C18 100 Å, LC Column 100 × 2.1 mm) using positive and negative mode electrospray ionization with a linear gradient of 5-95% acetonitrile (MeCN)-H_2O with 0.5% formic acid in 15 min followed by 95% MeCN for 5 min with a flow rate of 0.3 mL/min. Or LC-MS analyses were performed on a Shimadzu 2010 EV LC-MS (Phenomenex® Luna, 5 μm, 2.0 × 100 mm, C18 column) using positive and negative mode electrospray ionization with a linear gradient of 5-95% MeCN-H_2O with 0.5% formic acid in 30 minutes followed by 95% MeCN for 15 minutes with a flow rate of 0.1 mL/min. For large-scale analysis, the acetone extract from a 4 L SDA solid agar extract of *P. thymicola ΔpenF::PgpdA-asqC* mutant were evaporated to dryness and partitioned between ethyl acetate/H_2O three times. After evaporation of the organic phase, the crude extracts were separated by silica chromatography. The purity of each compound was checked by LC-MS, and the structure was confirmed by NMR. ^{1}H, ^{13}C and 2D NMR spectra were obtained using DMSO-d_6 as solvent on Bruker AV500 spectrometer with a 5 mm dual cryoprobe at the UCLA Molecular Instrumentation Center.

Protein expression and purification

Intron-free *penD* was inserted into plasmid pGEX 4T-1 to yield the pGEX4T-*penD*, which was transformed into *E. coli* BL21(DE3) strain for GST-PenD fusion protein expression. The *E. coli* BL21(DE3) cell harboring pGEX4T-*penD* was cultured in LB medium supplemented with 100 μg/mL ampicillin (final concentration) at 37°C and 250 rpm to OD_{600} of 0.5. The cultures were then incubated on ice for 10 min before addition of 0.2 mM (final concentration) IPTG to induce protein expression. The cells were further cultured at 16°C for 20 hours, and were harvested by centrifugation (3,500 rpm, 15 min, 4°C), resuspended in 40 mL buffer A (50 mM Tris-HCl, pH 7.9, 0.5 M NaCl, and 10% glycerol) and lysed by sonication on ice for 20 min. Cellular debris was removed by centrifugation (14,000 rpm, 45 min, 4°C), and the supernatant was used to purify the protein by GST-affinity chromatography using standard protocols. Protein concentration was determined by Bradford assay using bovine serum albumin as a standard, and the proteins were stored frozen at −80 °C.

Intron-free *penE* and *asqG* were inserted into the yeast expression plasmid pXW06 to yield the plasmids pXW06-*penE* and pXW06-*asqG* respectively. For expression of PenE and AsqG, the yeast cells harboring pXW06-*penE* or pXW06-*asqG* were grown in YPD medium supplemented with 2% dextrose at 28°C with shaking for 48 hours. The microsomes were prepared according to the protocol. Briefly, the cells were harvested by centrifugation (3,750 rpm at 4°C for 10 mins) and the cell pellet was washed with 100 mL of TES buffer (50 mM Tris-HCl, pH, 7.5, 1 mM EDTA, 0.6 M sorbitol). The cells were centrifuged as above, resuspended in 100 mL of TES-M (TES supplemented with 10 mM 2-mercaptoethanol), and allowed to incubate at room temperature for 10 min. The yeast cells were centrifuged again at 3,750 rpm for 10 min, and the pellet was resuspended in 2.5 mL of extraction buffer (1% bovine serum alb umin, fraction V, 2 mM 2-mercaptoethanol, 1 mM phenylmethylsulfonyl fluoride, all dissolved in TES). Zirconia/silica beads (0.5 mm in diameter, Biospec Products) were added until skimming the surface of the cell suspension. Cell walls were disrupted manually by hand shaking in a cold room for 10 min at 30-s intervals separated by 30-s intervals on ice. Cell extracts were transferred to a 50 mL centrifuge tube, the Zirconia/silica beads were washed three times with 5 mL of extraction buffer, and the washes were pooled with the original cell extracts. Finally, PenE and AsqG microsomes were obtained by differential centrifugation at 10,000g for 10 min at 4°C to remove cellular debris followed by centrifugation at 100,000g for 70 min at 4°C. The microsomal pellets were resuspended in 1.5 mL of TEG-M buffer (50 mM Tris-HCl, pH 7.5, 1 mM EDTA, 20% glycerol, and 1.5 mM 2-mercaptoethanol) and stored frozen at −80 °C.

Intron-free *penF, asqC* and *asqO* were inserted into the digestion sites *Spe*I/*Pml*I of yeast expression plasmid pXW55 to yield the plasmids pXW55-*penF,* pXW55-*asqC,* and pXW55-*asqO* respectively. These three proteins contain N-Flag Tag. For expression and purification of them, the yeast cells harboring pXW55-*penF,* pXW55-*asqC,* or pXW55-*asqO* were grown in YPD medium supplemented with 2% dextrose at 28°C with shaking for 48 hours. The cells were harvested by centrifugation (3,500 rpm, 20 minutes, 4°C), resuspended in 20 mL lysis buffer (50 mM NaH_2PO_4 pH 8.0, 0.15 M NaCl, 10 mM imidazole) and lysed through sonication on ice for 60 min. Cellular debris was removed by centrifugation (17,000 rpm, 60 min, 4°C). Purification of PenF, AsqC and AsqO through anti-FLAG affinity chromatography follows standard protocols (Sigma). Protein concentration was determined by Bradford assay using bovine serum albumin as a standard, and the proteins were stored frozen at −80 °C. The PenF and AsqO mutant proteins were following the same protocols.

Biotransformation assays

Intron-free *penJ* and *asqB* genes were cloned into plasmid pXW55 to yield the yeast-expression plasmids pXW55-*penJ* and pXW55-*asqB* respectively. i) pXW06-*penE*/pXW55-*penJ,* ii) pXW06-*asqG*/pXW55-*asqB,* iii) pXW06-*penE*/pXW55-*asqB,* or iv) pXW06-*asqG*/pXW55-*penJ* were transformed into *S. cerevisiae* BJ5464-NpgA strain. The transformants harboring different mFMO and hydrolase combinations (i-iv) were firstly grown in 2 mL uracil and L-tryptophan double drop-out medium at 28°C 1 day, and then they were transferred into 25 mL fresh YPD medium, and the cultures were shaken at 28°C, 250 rpm. 25 mL cultures were collected by centrifugation (4°C, 2000rpm, 10 min) after two days. The cell pellets were gently re-suspended in 1 mL fresh YPD medium, 200 μM **4** (final

concentration) was added, and then the cultures were shaken at 28°C, 250 rpm, 1 day for biotransformation. For product detection, cell cultures were extracted with 1 mL ethyl acetate two times. After evaporation of the organic phase, the crude extracts were dissolved in 300 °L methanol for LC-MS analysis.

In vitro characterization of PenE, PenF, PenD, AsqG, AsqC and AsqO

1) Assays for PenE and AsqG activity with **4** in 50 mM Tris-HCl (pH 7.4) buffer were performed at 100 μL scale with microsomal PenE or AsqG (from 20 mg/mL total protein concentration), 100 μM FAD, 0.4 mM NADPH, 28°C for 10 hours.

2) Assays for PenE and PenF or PenF E222A activity with **4** in 50 mM Tris-HCl (pH 7.4) buffer were performed at 100 μL scale with microsomal PenE (from 20 mg/mL total protein concentration), 20 μM PenF or PenF E222A, 100 μM FAD, 0.4 mM NADPH, 28°C for 10 hours.

3) Assays for PenE and PenF activity with **4** in 50 mM Tris-HCl (pH 7.4) buffer with EDTA were performed at 100 μL scale with microsomal PenE (from 20 mg/ml total protein concentration), 20 μM PenF, 100 μM FAD, 0.4 mM NADPH, 10 mM EDTA, 28°C for 10 hours.

4) Assays for PenE, PenF and PenD activity with **4** in 50 mM Tris-HCl (pH 7.4) buffer were performed at 100 μL scale with microsomal PenE (from 20 mg/ml total protein concentration), 20 μM PenF, 20 μM PenD, 100 μM FAD, 0.4 mM NADPH, 28°C for 10 hours.

5) Assays for PenD activity with **8** in 50 mM Tris-HCl (pH 7.4) buffer were performed at 100 μL scale with 20 μM PenD, 0.4 mM NADPH, 28°C for 10 hours.

6) Assays for AsqC activity with **4** in 50 mM Tris-HCl (pH 7.4) buffer were performed at 100 μL scale with 20 μM AsqC, 28°C for 10 hours.

7) Assays for AsqG activity with **9** in 50 mM Tris-HCl (pH 7.4) buffer were performed at 100 μL scale with microsomal PenG (from 20 mg/ml total protein concentration), 100 μM FAD, 0.4 mM NADPH, 28°C for 10 hours.

8) Assays for AsqG and AsqC activity with **4** in 50 mM Tris-HCl (pH 7.4) buffer were performed at 100 μL scale with microsomal AsqG (from 20 mg/mL total protein concentration), 20 μM AsqC, 100 μM FAD, 0.4 mM NADPH, 28°C for 10 hours.

9) Assays for AsqG and AsqO activity with **4** in 50 mM Tris-HCl (pH 7.4) buffer were performed at 100 μL scale with microsomal AsqG (from 20 mg/mL total protein concentration), 20 μM AsqO, 100 μM FAD, 0.4 mM NADPH, 28°C for 10 hours.

10) Assays for PenF or E222D and H220A activity with **10** in 50 mM Tris-HCl (pH 7.4) buffer were performed at 100 μL scale with 20 μM PenF or E222D and H220A, 28°C for 10 hours.

11) Assays for AsqO or AsqO D222A activity with **10** in 50 mM Tris-HCl (pH 7.4) buffer were performed at 100 μL scale with 20 μM AsqO or AsqO D222A, 28°C for 10 hours.

The reaction mixtures were quenched and extracted with 200 μL ethyl acetate (EA) two times. The resultant organic extracts were evaporated to dryness, re-dissolved in methanol, and then analyzed on LC-MS. LC-MS analyses were performed on a Shimadzu 2020 EV LC-MS (Kinetex™ 1.7 μm C18 100 Å, LC Column 100 × 2.1 mm) using positive and negative mode electrospray ionization with a linear gradient of 5-95% MeCN-H_2O with 0.5% formic acid in 15 minutes followed by 95% MeCN for 3 minutes with a flow rate of 0.3 mL/min.

BF_3·Et_2O catalyzes epoxide rearrangement of 10

To a stirred solution of **10** (5 mg, ~6.7 mmol) in dry THF (1.6 mL) was added BF_3·Et_2O (80 μL, ~0.64 mmol) at 0°C. The reaction mixture was stirred at room temperature for 2 hours. The reaction was quenched with saturated aqueous $NaHCO_3$ (3.2 mL) followed by extraction with EtOAc (3 × 6 mL). The crude product was purified by column chromatography to afford **12** as a yellow oil (~1.2 mg).

Computational details

Quantum mechanical calculations were performed using Gaussian 09 (Revision D.01).[48] All geometries were optimized using M06-2X,[49] within the IEFPCM model (water),[50] and the 6-31G(d) basis set. Single point energies were calculated using M06-2X,[49] within the IEFPCM model (water),[50] and the 6-311++G(d,p) basis set. The resulting energies were used to correct the gas phase energies obtained from the M06-2X optimizations.[51] Previous computational work on epoxide-opening cyclization reactions with similar methods provided results in accord with experiment.[14,15] Computed structures are illustrated with CYLView.[52] All calculations have been carried out using the model substrates based on compounds **5** and **10** (Supplementary Fig. 10).

Supplementary Material

Refer to Web version on PubMed Central for supplementary material.

ACKNOWLEDGMENTS

We thank Prof. Christian Hertweck for providing the standard of Aspoquinolone A/B (**2**). This work was supported by the NIH 1DP1GM106413 and 1R35GM118056 to YT; and the NSF CHE-1361104 to K.N.H. Computational resources were provided by the UCLA Institute for Digital Research and Education (IDRE) and the Extreme Science and Engineering Discovery Environment (XSEDE), which is supported by the NSF (OCI-1053575). M.G.-B thanks postdoctoral fellowship. K.W. thanks Japan Society for the Promotion of Science (JSPS) Program for Advancing Strategic International Networks to Accelerate the Circulation of Talented Researchers (No. G2604). We thank Profs. Michael Jung and Neil Garg, and Leibniz Hang for helpful discussions.

REFERENCES

1. Sienel, G., Rieth, R., Rowbottom, KT. Ullmann's Encyclopedia of Industrial Chemistry. Wiley-VCH Verlag GmbH & Co. KGaA; 2000. Epoxides..

2. Thibodeaux CJ, Chang WC, Liu HW. Enzymatic chemistry of cyclopropane, epoxide, and aziridine biosynthesis. Chem. Rev. 2012; 112:1681–1709. [PubMed: 22017381]
3. Jacobsen EN. Asymmetric catalysis of epoxide ring-opening reactions. Acc. Chem. Res. 2000; 33:421–431. [PubMed: 10891060]
4. Krake SH, Bergmeier SC. Inter- and intramolecular reactions of epoxides and aziridines with pi-nucleophiles. Tetrahedron. 2010; 66:7337–7360.
5. Pineschi M. Asymmetric ring-opening of epoxides and aziridines with carbon nucleophiles. Eur. J. Org. Chem. 2006; 22:4979–4988.
6. Schneider C. Synthesis of 1,2-difunctionalized fine chemicals through catalytic, enantioselective ring-opening reactions of epoxides. Synthesis. 2006; 23:3919–3944.
7. Smith JG. Synthetically Useful Reactions of Epoxides. Synthesis. 1984; 8:629–656.
8. Taylor SK. Reactions of epoxides with ester, ketone and amide enolates. Tetrahedron. 2000; 56:1149–1163.
9. Vilotijevic I, Jamison TF. Epoxide-opening cascades in the synthesis of polycyclic polyether natural products. Angew. Chem. Int. Edit. 2009; 48:5250–5281.
10. He J, Ling J, Chiu P. Vinyl epoxides in organic synthesis. Chem. Rev. 2014; 114:8037–8128. [PubMed: 24779795]
11. de Vries EJ, Janssen DB. Biocatalytic conversion of epoxides. Curr. Opin. Biotech. 2003; 14:414–420. [PubMed: 12943851]
12. Ueberbacher BT, Hall M, Faber K. Electrophilic and nucleophilic enzymatic cascade reactions in biosynthesis. Nat. Prod. Rep. 2012; 29:337–350. [PubMed: 22307731]
13. Dominguez de Maria P, van Gemert RW, Straathof AJ, Hanefeld U. Biosynthesis of ethers: unusual or common natural events? Nat. Prod. Rep. 2010; 27:370–392. [PubMed: 20179877]
14. Hotta K, Chen X, Paton RS, Minami A, Li H, Swaminathan K, et al. Enzymatic catalysis of anti-Baldwin ring closure in polyether biosynthesis. Nature. 2012; 483:355–358. [PubMed: 22388816]
15. Mao XM, Zhan ZJ, Grayson MN, Tang MC, Xu W, Li YQ, et al. Efficient biosynthesis of fungal polyketides containing the dioxabicyclo-octane ring System. J. Am. Chem. Soc. 2015; 137:11904–11907. [PubMed: 26340065]
16. Wendt KU, Schulz GE, Corey EJ, Liu DR. Enzyme mechanisms for polycyclic triterpene formation. Angew. Chem. Int. Edit. 2000; 39:2812–2833.
17. Tagami K, Liu C, Minami A, Noike M, Isaka T, Fueki S, et al. Reconstitution of biosynthetic machinery for indole-diterpene paxilline in *Aspergillus oryzae*. J. Am. Chem. Soc. 2013; 135:1260–1263. [PubMed: 23311903]
18. Tang MC, Lin HC, Li DH, Zou Y, Li J, Xu W, et al. Discovery of unclustered fungal indole diterpene biosynthetic pathways through combinatorial pathway reassembly in engineered yeast. J. Am. Chem. Soc. 2015; 137:13724–13727. [PubMed: 26469304]
19. Matsuda Y, Abe I. Biosynthesis of fungal meroterpenoids. Nat. Prod. Rep. 2016; 33:26–53. [PubMed: 26497360]
20. Archelas A, Furstoss R. Epoxide hydrolases: new tools for the synthesis of fine organic chemicals. Trends. Biotechnol. 1998; 16:108–116. [PubMed: 9523459]
21. Swanson PE. Dehalogenases applied to industrial-scale biocatalysis. Curr. Opin. Biotechnol. 1999; 10:365–369. [PubMed: 10449315]
22. Hammer SC, Marjanovic A, Dominicus JM, Nestl BM, Hauer B. Squalene hopene cyclases are protonases for stereoselective Bronsted acid catalysis. Nat. Chem. Biol. 2015; 11:121–126. [PubMed: 25503928]
23. Rickborn, B. 3.3 - Acid-catalyzed Rearrangements of Epoxides. In: Trost, Barry M., Fleming, I., editors. Comprehensive Organic Synthesis. Pergamon; Oxford: 1991. p. 733-775.
24. Jung ME, D'Amico DC. Stereospecific rearrangement of optically active tertiary allylic epoxides to give optically active quaternary aldehydes: synthesis of .alpha.-alkyl amino aldehydes and acids. J. Am. Chem. Soc. 1995; 117:7379–7388.
25. Meninno S, Lattanzi A. Organocatalytic asymmetric reactions of epoxides: recent progress. Chemistry. 2016; 22:3632–3642. [PubMed: 26785400]

26. Song ZL, Fan CA, Tu YQ. Semipinacol rearrangement in natural product synthesis. Chem. Rev. 2011; 111:7523–7556. [PubMed: 21851053]
27. Corey EJ, Guzman-Perez A. The catalytic enantioselective construction of molecules with quaternary carbon stereocenters. Angew. Chem. Int. Edit. 1998; 37:388–401.
28. Scherlach K, Hertweck C. Discovery of aspoquinolones A-D, prenylated quinoline-2-one alkaloids from *Aspergillus nidulans*, motivated by genome mining. Org. Biomol. Chem. 2006; 4:3517–3520. [PubMed: 17036148]
29. Uchida R, Imasato R, Yamaguchi Y, Masuma R, Shiomi K, Tomoda H, et al. Yaequinolones, new insecticidal antibiotics produced by Penicillium sp. FKI-2140. I. Taxonomy, fermentation, isolation and biological activity. J. Antibiot (Tokyo). 2006; 59:646–651. [PubMed: 17191680]
30. Uchida R, Imasato R, Tomoda H, Omura S. Yaequinolones, new insecticidal antibiotics produced by Penicillium sp. FKI-2140. II. Structural elucidation. J. Antibiot (Tokyo). 2006; 59:652–658. [PubMed: 17191681]
31. Zou Y, Zhan Z, Li D, Tang M, Cacho RA, Watanabe K, et al. Tandem prenyltransferases catalyze isoprenoid elongation and complexity generation in biosynthesis of quinolone alkaloids. J. Am. Chem. Soc. 2015; 137:4980–4983. [PubMed: 25859931]
32. Trofast J, Wickberg B. Mycorrhizin a and chloromycorrhizin a, two antibiotics from a mycorrhizal fungus of *monotropa hypopitys* L. Tetrahedron. 1977; 33:875–879.
33. Simonetti SO, Larghi EL, Kaufman TS. The 3,4-dioxygenated 5-hydroxy-4-aryl-quinolin-2(1H)-one alkaloids. Results of 20 years of research, uncovering a new family of natural products. Nat. Prod. Rep. 2016 DOI: 10.1039/C6NP00064A.
34. Ishikawa N, Tanaka H, Koyama F, Noguchi H, Wang CC, Hotta K, et al. Non-heme dioxygenase catalyzes atypical oxidations of 6,7-bicyclic systems to form the 6,6-quinolone core of viridicatin-type fungal alkaloids. Angew. Chem. Int. Edit. 2014; 53:12880–12884.
35. Hiseni A, Otten LG, Arends IW. Identification of catalytically important residues of the carotenoid 1,2-hydratases from Rubrivivax gelatinosus and Thiocapsa roseopersicina. Appl. Microbiol. Biotechnol. 2015; 100:1275–1284.
36. Thoma R, Schulz-Gasch T, D'Arcy B, Benz J, Aebi J, Dehmlow H, et al. Insight into steroid scaffold formation from the structure of human oxidosqualene cyclase. Nature. 2004; 432:118–122. [PubMed: 15525992]
37. Jung ME, Piizzi G. Gem-disubstituent effect: theoretical basis and synthetic applications. Chem. Rev. 2005; 105:1735–1766. [PubMed: 15884788]
38. Yu B, Jiang T, Quan W, Li J, Pan X, She X. An efficient method for construction of the angularly fused 6,3,5-tricyclic skeleton of mycorrhizin A and its analogues. Org. Lett. 2009; 11:629–632. [PubMed: 19175348]
39. Narjes F, Bolte O, Icheln D, Koenig WA, Schaumann E. Synthesis of vinylcyclopropanes by intramolecular epoxide ring opening. Application for an enantioselective synthesis of dictyopterene A. J. Org. Chem. 1993; 58:626–632.
40. White JD, Jensen MS. Cyclopropane-containing eicosanoids of marine origin. Biomimetic synthesis of constanolactones A and B from the alga *Constantinea simplex*. J. Am. Chem. Soc. 1995; 117:6224–6233.
41. Ahmed SA, Simpson TJ, Staunton J, Sutkowski AC, Trimble LA, Verderas JC. Biosynthesis of aspyrone and asperlactone, pentaketide metabolites of Aspergillus melleus. Incorporation studies with [1-^{13}C, $^{18}O_2$]acetate and $^{18}O_2$ gas. J. Chem. Soc., Chem. Commun. 1985; 23:1685–1687.
42. Yang YL, Zhou H, Du G, Feng KN, Feng T, Fu XL, et al. A monooxygenase from *Boreostereum vibrans* catalyzes oxidative decarboxylation in a divergent vibralactone biosynthesis pathway. Angew. Chem. Int. Edit. 2016; 55:5463–5466.
43. Li S, Finefield JM, Sunderhaus JD, McAfoos TJ, Williams RM, Sherman DH. Biochemical characterization of NotB as an FAD-dependent oxidase in the biosynthesis of notoamide indole alkaloids. J. Am. Chem. Soc. 2012; 134:788–791. [PubMed: 22188465]
44. Tsunematsu Y, Ishikawa N, Wakana D, Goda Y, Noguchi H, Moriya H, Hotta K, Watanabe K. Distinct mechanisms for spiro-carbon formation reveal biosynthetic pathway crosstalk. Nat. Chem. Biol. 2013; 9:818–825. [PubMed: 24121553]

45. Wendt KU, Poralla K, Schulz GE. Structure and function of a squalene cyclase. Science. 1997; 277:1811–1815. [PubMed: 9295270]

46. Boutaud O, Ceruti M, Cattel L, Schuber F. Retention of the label during the conversion of (3-3H)squalene into (3S)-2,3-oxidosqualene catalyzed by mammalian squalene oxidase. Biochem. Biophys. Res. Commun. 1995; 208:42–47. [PubMed: 7887959]

47. Condon BJ, Leng Y, Wu D, Bushley KE, Ohm RA, Otillar R, et al. Comparative genome structure, secondary metabolite, and effector coding capacity across Cochliobolus pathogens. PLoS. Genet. 2013; 9:e1003233. [PubMed: 23357949]

ONLINE METHONDS REFERENCES

48. Frisch, MJ., Trucks, GW., Schlegel, HB., Scuseria, GE., Robb, MA., Cheeseman, JR., et al. Wallingford, CT, USA: 2009.

49. Zhao Y, Truhlar DG. The M06 suite of density functionals for main group thermochemistry, thermochemical kinetics, noncovalent interactions, excited states, and transition elements: two new functionals and systematic testing of four M06-class functionals and 12 other functionals. Theor. Chem. Acc. 2008; 120:215–241.

50. Tomasi J, Mennucci B, Cammi R. Quantum mechanical continuum solvation models. Chem. Rev. 2005; 105:2999–3093. [PubMed: 16092826]

51. Simon L, Goodman JM. How reliable are DFT transition structures? Comparison of GGA, hybrid-meta-GGA and meta-GGA functionals. Org. Biomol. Chem. 2011; 9:689–700. [PubMed: 20976314]

52. Legault C. Université de Sherbrooke, Sherbrooke, Quebec, Canada. 2009

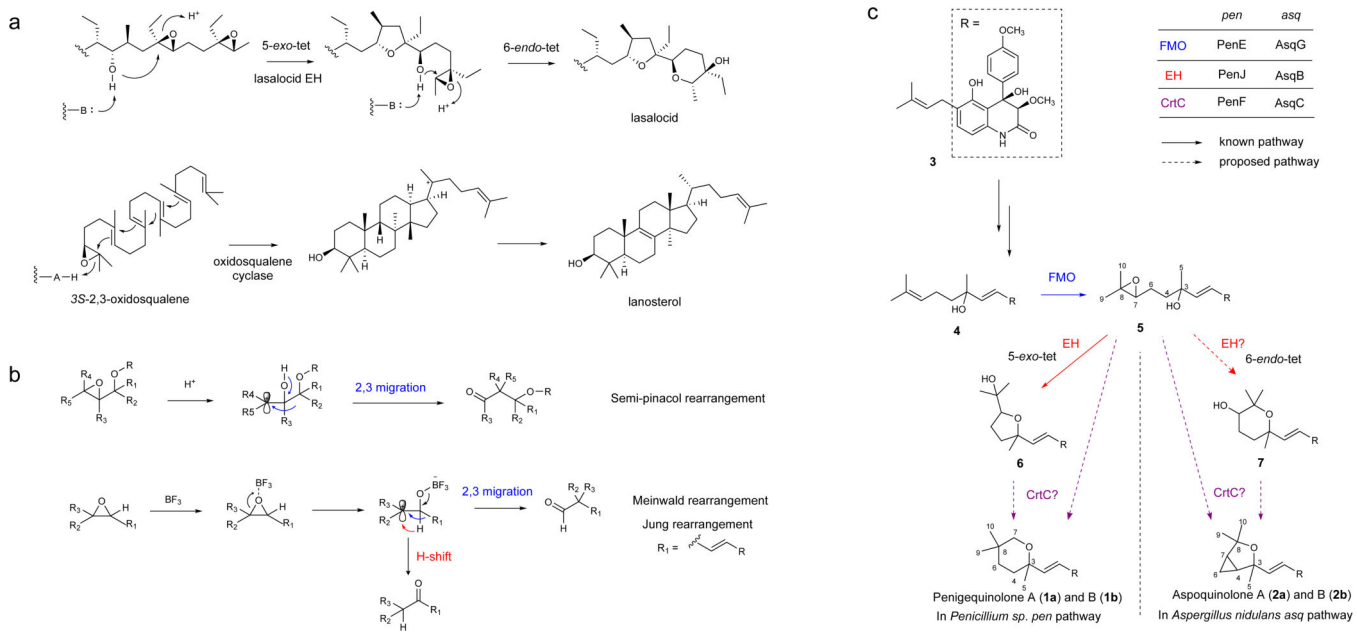

Figure 1. Versatility of epoxide as a (bio)synthon and the quinolone alkaloid biosynthetic pathways

(**a**) Biosynthetic reactions using epoxide as a biosynthon. Examples shown are for lasalocid and lanosterol formation catalyzed by epoxide hydrolase and oxidosqualene cyclase, respectively. (**b**) The cationic rearrangement of epoxide under strongly acidic conditions in organic synthesis. The semi-pinacol, Meinward and Jung rearrangements all involve the formation of a carbocation intermediate followed by C-C bond migration to yield aldehydes or ketones. A comparable reaction has not been reported in Nature. (**c**) Knowledge of the quinolone alkaloid biosynthetic pathways at the onset of this study. Penigequinolone A (**1a**) and B (**1b**) are from the *pen* pathway in *Penicillium sp.,* while aspoquinolone A (**2a**) and B (**2b**) are from the *asq* pathway in *Aspergillus nidulans.* The alcohol **4** is oxidized into the epoxide **5** by the FMO in the pathways, which can spontaneously form the 5-*exo*-tet product **6**. Previously, **1** was proposed to derive from **6**, while **2** was proposed to derive from the 6-*endo*-tet product **7**. The common uncharacterized genes in the two pathways are shown, and the two CrtC enzymes were investigated in this work to possibly catalyze the formation of **1** and **2** from either **6**, **7**, or **5**.

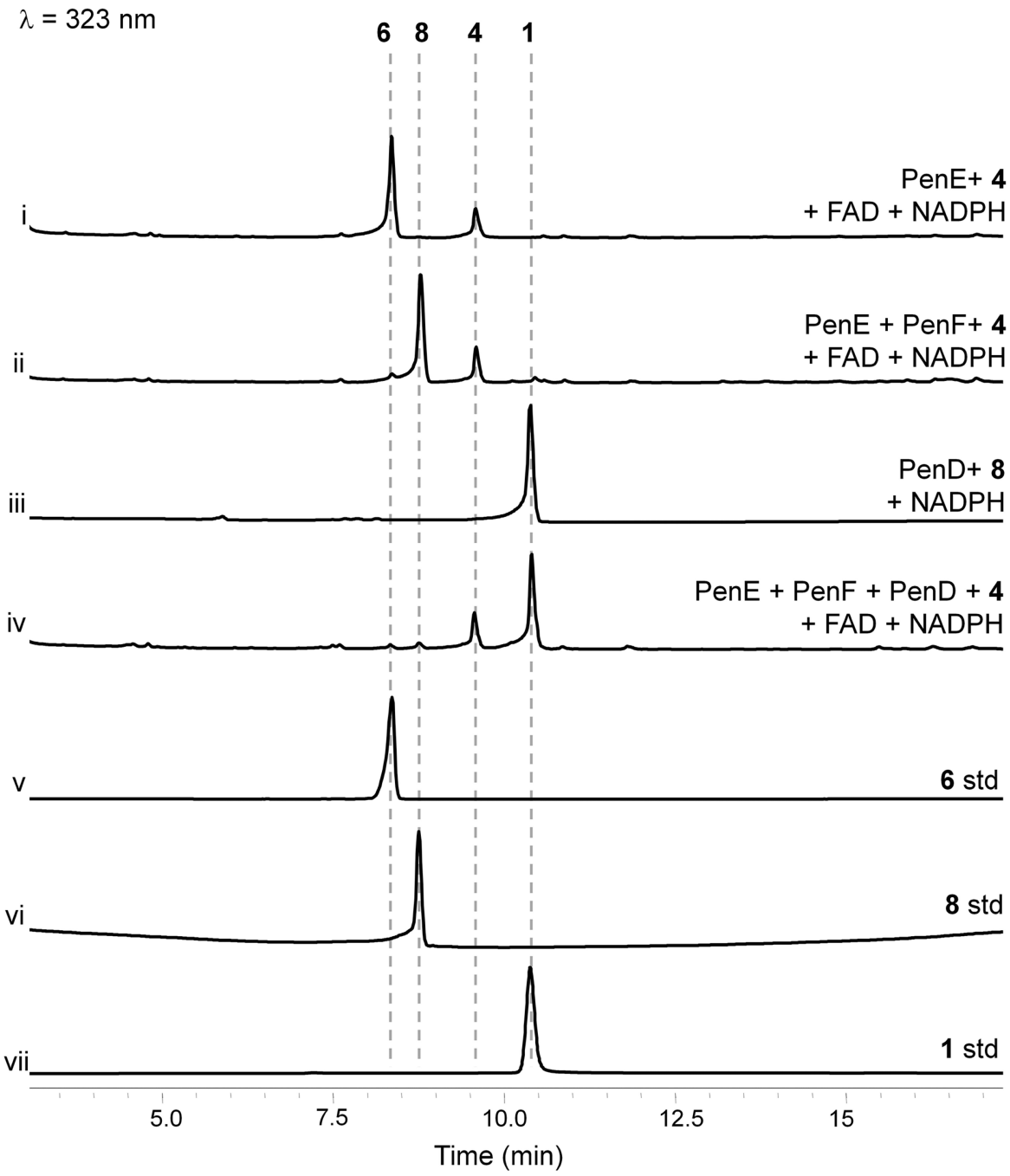

Figure 2. In vitro reconstitution of the conversion of 5 to 1

Since **5** cannot be stably isolated given its rapid conversion to **6**, a coupled assay using PenE and **4** were performed. The assays demonstrate PenF can convert **5** to hemiacetal **8**, which is dehydrated and reduced to **1** by the SDR-like reductase PenD.

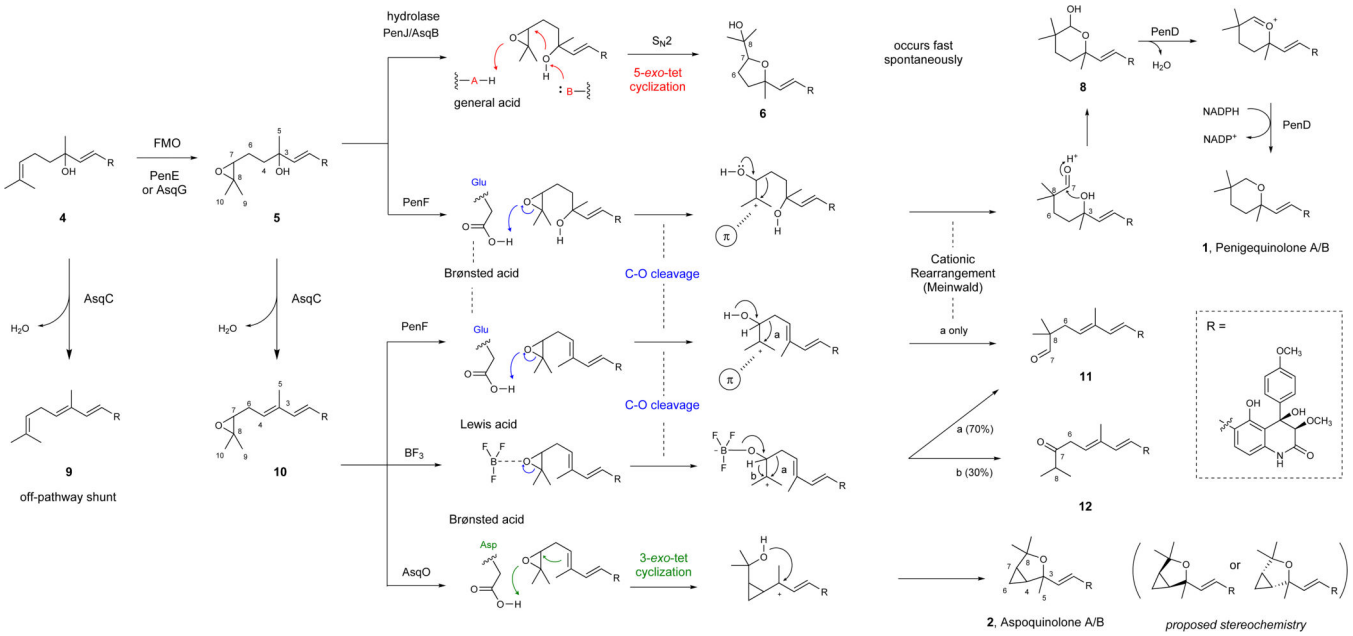

Figure 3. Proposed reactions catalyzed by PenF and AsqO on the epoxide substrates

AsqC catalyzes the dehydration of **5** to yield the stable **10**, as well as that of **4** to yield the shunt product **9**. The 5-*exo*-product **6** is proven to be an off-pathway product in the absence of PenF. PenF catalyzes the cationic rearrangement of epoxides **5** and **10** to yield the corresponding aldehydes. Both the aldehyde **11** and ketone **12** can be formed from **10** in the presence of $BF_3{\cdot}Et_2O$. In sharp contrast to PenF, AsqO catalyzes the formation of **2** from **10** via a 3-*exo*-tet cyclization. We propose revision of the stereochemistry of **2** to be either pair of diastereomers shown in parentheses.

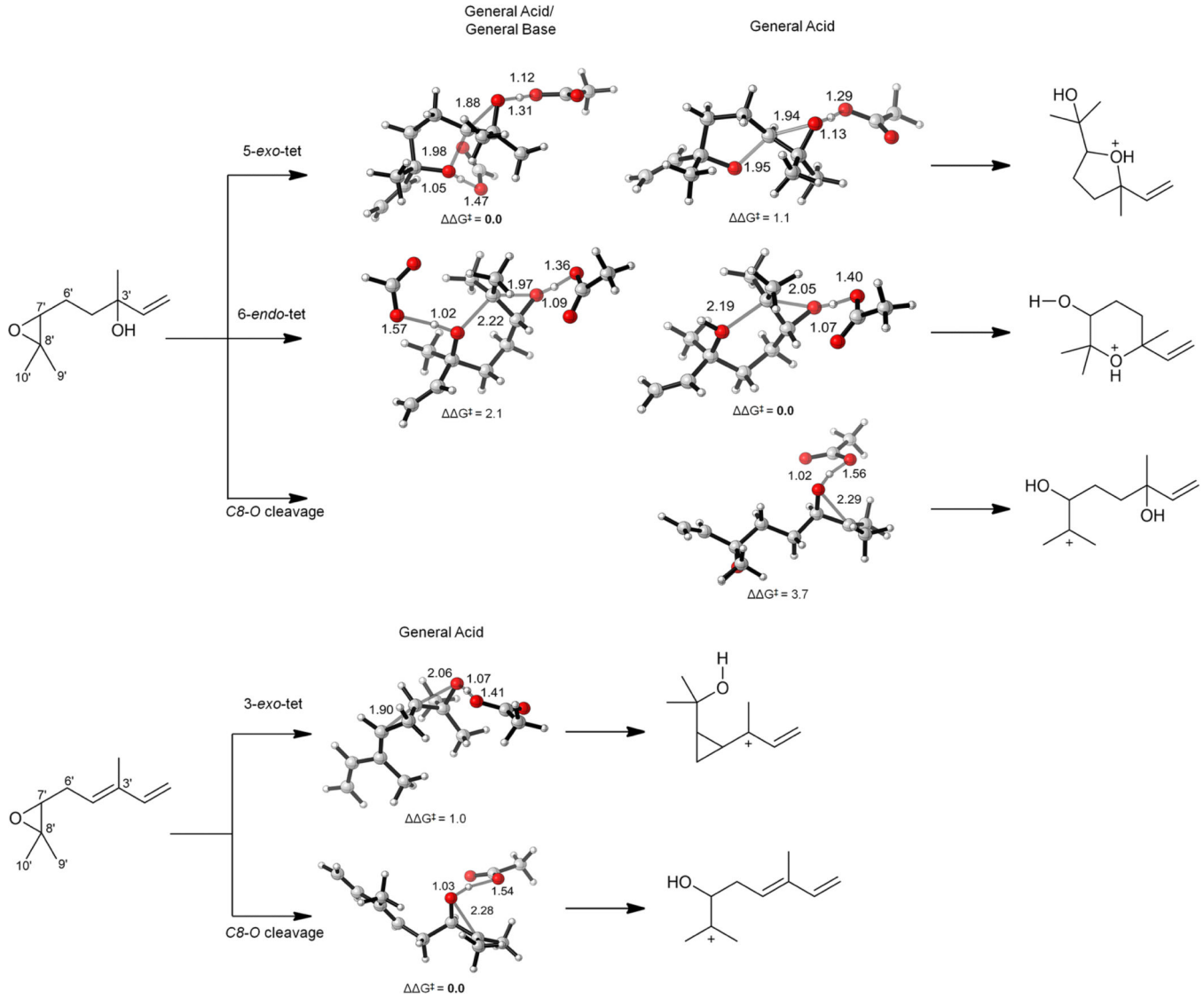

Figure 4. Computational studies on model epoxides

(a) General acid and general acid/general base catalyzed 5-*exo* and 6-*endo* cyclization and C8-O cleavage of a model for epoxide **5**. **(b)** General acid catalyzed 3-*exo* and C8-O cleavage of a model for epoxide **10**. Lowest-energy transition state (TS) structures calculated at M06-2X/6-311++G(d,p)-IEFPCM(water)//M06-2X/6-31G(d)-IEFPCM(water) level, activation free energies (kcal mol^{-1}), and forming/breaking bond distances (in Ångstroms) are given.

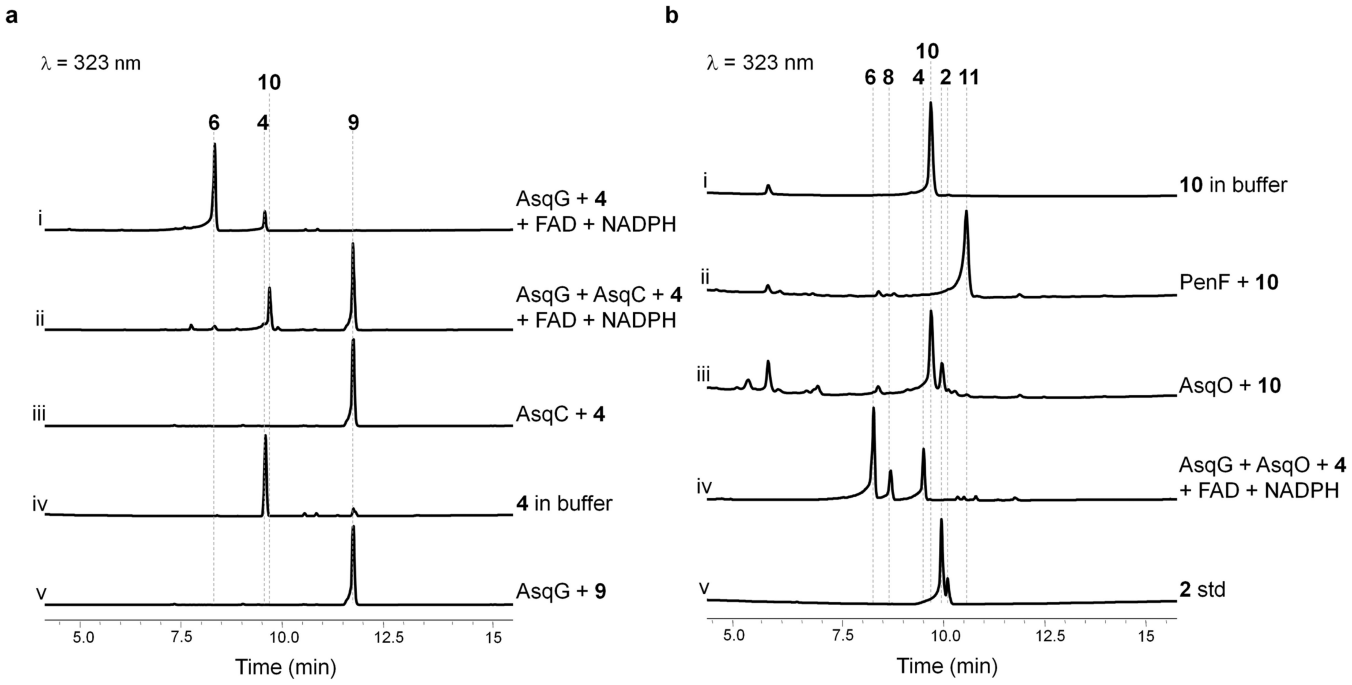

Figure 5. In vitro reconstitution of activities of *asq* enzymes and enzymatic synthesis of 2

(**a**) Confirming the activity of AsqC as a dehydratase in the *asq* pathway. Comparison of substrate promiscuity of AsqC and AsqG showed AsqG functions upstream of AsqC, and **10** is the on-pathway product. (**b**) AsqO, a second CrtC enzyme in the *asq* cluster, catalyzes the 3-*exo*-tet reaction of **10** to yield **2**. In contrast, PenF converts **10** to **11** via a cationic rearrangement, further confirming its unique activity.